

we feel bear the closest resemblance to the fcc thallos halides, have an effective charge of $0.68e$.¹² So we assume $0.86e$ and $0.68e$ to be upper and lower bounds for the unknown effective charges. Putting all these values together we end up with a static dielectric constant of fcc thallos halides in the range of 10 to 15.

The calculated effective masses, which also influence the exciton binding energy, are larger than in the sc structure, namely $m_e = 0.4m_0$ (0.3), $m_h = 0.6m_0$ (0.5) for TlCl and $m_e = 0.4m_0$ (0.2), $m_h = 0.65m_0$ (0.4) for TlBr; the sc values⁶ are given in parentheses. This increase together with the aforementioned drastic decrease in ϵ_0 and ϵ_∞ results in exciton binding energies in the range from 60 to 100 meV and effective hydrogenic radii of 12 to 16 Å.¹³ These values explain the experimentally observed sharpness and stability of the first exciton peak against rising temperature and decreasing layer thickness, as well as the existence of further sharp structure in the direct neighborhood of the first excitonic peak. A precise assignment of peaks α and β as due to either the 2s exciton or the valley-orbit partner of the 1s exciton is as yet impossible. Clarification is planned through absorption measurements in electric and magnetic fields and under external strain.

In conclusion we have shown that the optical properties and the electronic structure of fcc TlCl and TlBr differ quite markedly from their simple-cubic counterparts, and that this difference is a consequence of the different type of binding and not of microcrystallite or layer effects or the influence of the chemical nature of the substrate.

Thanks are due to Dr. H. Kappert for performing the electron-diffraction measurements, and

to J. Pollmann and Professor D. Fröhlich for fruitful discussions.

¹R. Z. Bachrach and F. C. Brown, Phys. Rev. B 1, 818 (1970).

²S. Kurita and K. Kobayashi, J. Phys. Soc. Jpn. 30, 1645 (1971).

³D. Fröhlich, J. Treusch, and W. Kottler, Phys. Rev. Lett. 29, 1603 (1972).

⁴E. Mohler, G. Schlögl, and J. Treusch, Phys. Rev. Lett. 27, 424 (1971).

⁵R. Shimizu, T. Koda, and T. Murashi, J. Phys. Soc. Jpn. 36, 161 (1974).

⁶H. Overhof and J. Treusch, Solid State Commun. 9, 53 (1971).

⁷L. G. Schultz, Acta Crystallogr. 4, 487 (1951).

⁸S. Tutihasi, J. Phys. Chem. Solids 12, 344 (1960).

⁹H. Overhof and U. Rössler, Phys. Status Solidi 37, 691 (1970).

¹⁰E.g., L. Pauling, *The Nature of the Chemical Bond and the Structure of Molecules and Crystals* (Cornell Univ. Press, Ithaca, N. Y., 1960); M. P. Tosi, in *Solid State Physics*, edited by H. Ehrenreich, F. Seitz, and D. Turnbull (Academic, New York, 1964), Vol. 16, p. 1.

¹¹As a matter of fact, for 200-Å layers of TlCl with a strongly disturbed sc structure a transition was measured at 3.2 eV, which is assigned to the X-R indirect transition of sc TlCl; K. Heidrich and W. Staude, in Proceedings of the Spring Meeting of the German Physical Society, Freudenstadt, Germany, 1974 (unpublished).

¹²R. P. Lowndes and D. H. Martin, Proc. Roy. Soc., Ser. A 308, 473 (1969).

¹³These values are calculated, by using Haken's potential, with an improved perturbation treatment, proposed by J. Pollmann, Phys. Status Solidi (b) 63, 548 (1974), which for sc TlCl yields a value of 7.7 meV for the exciton binding energy in reasonable accordance with experiment, the effective hydrogenic radius being 45 Å.

Structural Anomalies in Cubic (A15) V₃Si and Nb₃Sn

C. M. Varma, J. C. Phillips, and S.-T. Chui

Bell Laboratories, Murray Hill, New Jersey 07974

(Received 9 September 1974)

A variety of anomalous properties of A15 compounds can be explained by assuming that the perfect lattices become unstable at low temperatures, but are stabilized by small distortions around point defects which increase with decreasing temperature. In particular, the presence of vacancies explains discrepancies between sound-velocity measurements and recent lattice-constant measurements as a function of pressure.

The highest superconducting transition temperatures T_c which have been observed so far are found in intermetallic compounds A_3B , where A

is one of the transition metals Nb or V, and B is a metal or metalloid (e.g., Ga, Si, Ge, or Sn). A number of structural anomalies have been ob-

served to be correlated with high- T_c superconductors (which need not have the A15 structure), and it is generally believed that these structural anomalies arise because of unusually strong electron-phonon interactions; the latter must eventually place an upper limit¹ on physically attainable values of T_c .

While it is clear that a variety of microscopic factors contribute to the electron-phonon interaction, for some time experimentalists have hoped that, given a wide range of superconducting compounds and alloys, the ones with the highest values of T_c will share a specific kind of structural anomaly. For this reason there have been a number of attempts to identify the microscopic nature of the limiting structural anomaly for cubic A15 compounds. In general, two kinds of superconductive lattice instabilities have been observed: (1) a macroscopic instability associated with a cubic-to-tetragonal lattice distortion² specific to A15 compounds, and (2) more generally, microscopic instabilities in the phonon spectrum,³ i.e., anomalies in $\omega(q)$. In each crystal family the metals with the highest values of T_c show⁴ the largest anomalies in $\omega(q)$.

The (so far as we know) microscopically characteristic feature of the (A15) A_3B compounds is that at least one of the anomalies in $\omega(q)$ occurs for q near zero and it is associated with [110] TA phonons. Because the symmetry of these soft phonons is consistent with the macroscopic shear of the cubic-to-tetragonal phase transformation, it is tempting to suppose that the microscopic and macroscopic stabilities are somehow related. While one can construct electronic models which explain the macroscopic transition via a Jahn-Teller Fermi-surface mechanism,⁵ these microscopic models are not quite satisfactory when compared with microscopic neutron scattering data.⁶ Not only do they contain no mechanism for explaining the "central peak," but they must also invoke⁶ a separate complex Fermi-surface mechanism to explain the "kink" in the [110] TA $\omega(q)$ curve. Moreover, the separation of $\omega(q)$ into two linear parts, with the $q > q_0$ part behaving like⁶

$$\omega^2(q, T) \cong \omega^2(q, 300^\circ\text{K}) - aT^2, \quad (1)$$

is not consistent with the usual "dip" only near q_0 found in connection with Fermi-surface anomalies. These typically occur for values of q_0 of order a sizable fraction of a reciprocal-lattice vector, rather than the rather small value {about $0.09(\vec{G}/z)$, where \vec{G} is the [200] reciprocal-lattice vector} which is found⁶ in Nb_3Sn .

These difficulties in reconciling macroscopic with microscopic anomalies led some of us to propose⁷ that as the temperature is lowered the medium-range interatomic forces become sufficiently attractive that the [110] TA modes near $q=0$ become unstable $\{\omega_{\text{TA}}^2(q) < 0$ for q along [110] and $q < q_1$; the relationship between q_1 and q_0 is discussed below}. It is then suggested that this macroscopic instability is resolved by microscopic distortions around vacancies and by ordering of vacancies as T is lowered. Because the effects of vacancies cannot be treated by perturbation theory, a two-dimensional model was analyzed numerically⁸ with the results shown, for the reader's convenience, in Fig. 1. The model consisted of a square lattice with, for computational convenience, a square superlattice of vacancies (1% concentration). The dispersion curves shown in Fig. 1 are for the relaxed (stable) lattice in the presence of the vacancies. As the medium-range force parameter a' becomes more negative, the lattice without vacancies becomes more unstable, and the dispersion curves develop a kink near q_0 , strongly reminiscent of that observed⁶ in Nb_3Sn . The discontinuity in the sound velocity (as distinguished from a gradual

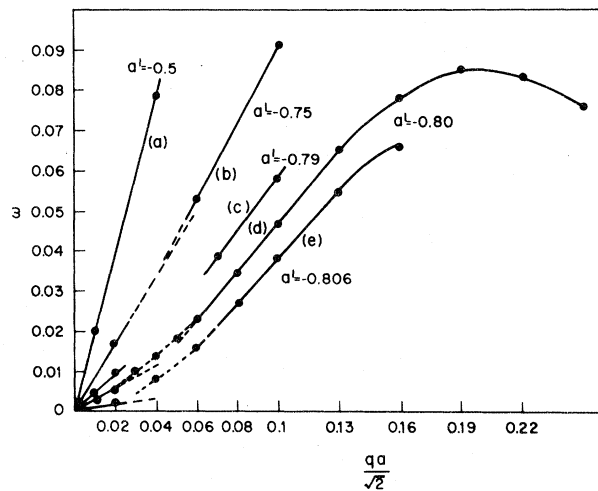


FIG. 1. Dispersion curves of a two-dimensional, soft, perfect-square lattice $\{\omega^2(q) < 0$ for $q < q_0\}$ which has been stabilized by addition of $c = 0.01$ vacancies. The curves shown correspond to different values of a medium-range force parameter a' ; the perfect lattice would be unstable ($q_0 > 0$) for $a' < -0.75$. While it is somewhat unphysical to fix c while varying a' (which is somewhat analogous to fixing c while varying the temperature T), there is a striking resemblance between the dispersion curves of Fig. 4 in Ref. 6 and the calculated curves shown here.

dispersive effect) is also contained in this model. The calculations suggest⁸ that the kink wave number q_0 depends both on the average vacancy spacing λ_0 and the range λ_1 of the attractive forces responsible for lattice softening and may be taken for simplicity as

$$2\pi/q_0 \cong \lambda_0 + \lambda_1. \quad (2)$$

Thus q_0 gives an upper limit on the vacancy concentration.

Although the vacancy mechanism can explain the observed⁶ phonon kink, an independent test of the presence of vacancies is desirable. This is provided by recent studies⁹ of the lattice structure of V_3Si under pressure at room temperature. These studies were carried out in the hope of observing at $(p, 300^\circ K)$ the macroscopic cubic-to-tetragonal instability which had been suggested at $(0, T < 80^\circ K)$ by measurements¹⁰ of the $[110]$ shear modulus C_s . When $-\Delta a/a$ is plotted against p , again two linear portions with a kink near 10 kbar are found, with the low- p slope disagreeing with the bulk modulus as deduced by sound-velocity measurement¹⁰ and with the high- p line extrapolating at $p=0$ to $-\Delta a/a = (1-2) \times 10^{-3}$, corresponding to a vacancy concentration in V_3Si of about 1% which is "squeezed out" altogether by a pressure of about 10 kbar. This estimate is arrived at by assuming that the relaxation volume associated with a vacancy is about the same as the volume apportioned to the atom. The concentration of ordered vacancies suggested by (2) in Nb_3Sn is about 1%, so that the model is qualitatively consistent for the two related materials. It is difficult to think of another model which would qualitatively give rise to the "kink" in $\Delta a/a$.

The vacancy model also resolves the paradox in the behavior of $-\Delta a/a$ versus pressure at low pressures. The slope at high pressure is that given by

$$-\frac{\Delta a}{a} = -\frac{1}{3} \frac{\Delta V}{V_0} = -\frac{1}{3} \frac{p}{V_0} \frac{dV}{dp}, \quad (3)$$

$$\begin{aligned} \frac{dV}{dp} &= \left. \frac{\partial V}{\partial p} \right|_c + \Delta V_0 \frac{\partial c}{\partial p} \text{ for } 0 \leq p \leq p_0, \\ &= \left. \frac{\partial V}{\partial p} \right|_c, \quad p \geq p_0, \end{aligned} \quad (4)$$

where p_0 is the pressure at which all the vacancies are squeezed out and ΔV_0 is the volume change per vacancy. The term $(dV/dp)_c$ is measured in the typical sound-velocity experiment (frequency of order 10^6 Hz), while da/dp is measured in a lattice-constant (static) measurement.

A separate static measurement of dV/dp is expected to exhibit a somewhat larger "kink" at p_0 because it includes the vacancy volume as well as the relaxation volume.

Using a simple model for vacancy energetics,

$$E = \alpha(p, T)c + \frac{1}{2}\beta(p, T)c^2, \quad (5)$$

and taking $\beta > 0$ so that vacancies have a tendency to order (rather than segregate), and $\alpha(p, T) = \Delta(T)(p - p_0)$ for $p < p_0$, one can deduce from the experimental results that $\Delta p_0/\beta \approx 5 \times 10^{-2}$ at room temperature. Further Δ is of the order of the volume for a vacancy, which we may take to be the volume usually apportioned to the metal atom. We then have an estimate of about 1000 K for the energy $-\alpha$ of a vacancy in V_3Si at STP. If Δ increases with decreasing temperature, then essentially all the phonon frequencies (not just the critical mode) will decrease. This is consistent with the experimental results [e.g., Eq. (1)] and our basic proposition that the greater the tendency of the pure crystal to be unstable, the larger the concentration of vacancies in an actual crystal.

Independent evidence¹¹ is available that the defect energies in V_3Ga (also of the A15 type) are anomalously small. This is provided by the enormous change in ductility in pressures as low as 10 kbar.

Associated with a tetragonally unstable perfect lattice which contains point defects are microscopically tetragonal $[011]$ domains around each defect; the further orientational ordering of these domains can give rise to a macroscopic $[001]$ low-temperature, cubic-to-tetragonal lattice deformation at $T = T_m$, as well as a narrow quasi-elastic "central" peak in neutron scattering.⁵ It can also be used to explain qualitatively anomalously large second-harmonic generation,¹² in macroscopically cubic V_3Si . [Incidentally, the large (symmetry forbidden in cubic crystals) second-harmonic generation at 50 K is indirect evidence of the continued presence of vacancies at low temperatures.] Additional evidence of the noncubic behavior of the A15 compounds above the macroscopic transformation temperature is available from thermal-expansion measurements.¹³

In conclusion, it appears that the preponderance of experimental evidence to date supports a specific model for the mechanism which opposes the lattice instabilities of high- T_c (A15) superconductors. This model consists of distorted microstructures centered on point defects (with long-range order). Such a model is attractive

because it is consistent with a number of empirical rules¹⁴ for high- T_c superconductors. The mechanism seems to be particularly well suited to binary compounds, and it may explain why some, otherwise promising (and very novel), intermetallic ternary compounds¹⁴ (such as $X_{0.5}Mo_3S_4$) have not produced T_c 's as high as have been found in the A15 family. We also note that enhancement of T_c associated with suppression of a superlattice instability (possibly analogous to the vacancy superlattices discussed here for the cubic A15 compounds) has recently been observed¹⁵ in hexagonal MoN, and that Mo clustering enhances T_c in many Mo compounds.¹⁵

For V_3Si the point defects are probably vacancies because of the anomaly⁹ in da/dp and because $dT_c/dp > 0$ and $dT_m/dp < 0$.¹⁶ However, antistructure defects (A atoms on B sites and vice versa) are plausible candidates for the predominant point defects in Nb_3Sn because R_B/R_A is larger there than in V_3Si (here R is the conventional metallic radius and *not* the Geller radius¹⁷). Under pressure the concentration of antistructure defects should increase, because the interchange of A and B atoms weakens the covalency of the A chains and thereby produces (on an atomic scale) a transition similar to the covalent-metallic transition observed in diamond-type crystals under pressure.¹⁸ The increasing concentration of antistructure defects with pressure in Nb_3Sn gives $dT_c/dp < 0$ and $dT_m/dp > 0$, in agreement with experiment.¹⁹ Large concentrations of antistructure defects are thought to have been produced in Nb_3B ($B=Al, Ga, Ge, \text{ and } Sn$) by giant neutron fluences.²⁰

To distinguish the two types of point defects, positron-annihilation experiments may identify vacancies, while the simplest system which exhibits both a microscopic anomaly in $\omega(q)$ and macroscopic anomalies in $\partial T_c/\partial p$, similar to those found in the A15 compounds, is Nb and its alloys.²¹ The TA modes for \vec{q} near zero and along a [100] axis exhibit softening,³ but less severely than Nb_3Sn . From alloy data²¹ on $\partial T_c/\partial p$ one may infer that if vacancies help to stabilize Nb, then their concentration may reach a maximum in $Nb_{1-x}Zr_x$ alloys for x near 0.15. Studies of da/dp as a function of p in these alloys would be of interest, and might reveal anomalies simi-

lar to those found⁹ in V_3Si .

We wish to acknowledge several stimulating conversations with Dr. L. R. Testardi.

¹H. Fröhlich, Phys. Lett. **A35**, 325 (1971), and Proc. Roy. Soc., Ser. A **215**, 291 (1952).

²B. W. Batterman and C. S. Barrett, Phys. Rev. Lett. **13**, 370 (1964), and Phys. Rev. **145**, 296 (1966); R. Mailfort, B. W. Batterman, and J. J. Hanak, Phys. Lett. **24A**, 315 (1967); L. R. Testardi and T. B. Bateman, Phys. Rev. **154**, 402 (1967).

³B. N. Brockhouse *et al.*, Phys. Rev. **128**, 1099 (1962); Y. Nakagawa and A. D. B. Woods, Phys. Rev. Lett. **11**, 271 (1963).

⁴H. G. Smith, in *Superconductivity in d- and f-Band Metals*, AIP Conference Proceedings No. 4, edited by D. H. Douglass (American Institute of Physics, New York, 1972).

⁵J. Labbé and J. Friedel, J. Phys. (Paris) **27**, 153 (1966); J. Labbé, Phys. Rev. **172**, 451 (1968).

⁶G. Shirane and J. D. Axe, Phys. Rev. Lett. **27**, 1083 (1971); J. D. Axe and G. Shirane, Phys. Rev. B **8**, 1965 (1973).

⁷S.-T. Chui and J. C. Phillips, Bull. Amer. Phys. Soc. **19**, 365 (1974).

⁸S.-T. Chui, to be published.

⁹R. D. Blaugher, A. Taylor, and M. Ashkin, Phys. Rev. Lett. **33**, 292 (1974).

¹⁰L. R. Testardi, Phys. Rev. B **5**, 4342 (1972); P. F. Garcia, G. R. Barsch, and L. R. Testardi, Phys. Rev. Lett. **27**, 944 (1971).

¹¹Ye. D. Martynov *et al.*, Fiz. Metal. Metalloved. **24**, 522 (1967).

¹²L. Testardi, Phys. Rev. Lett. **31**, 37 (1973).

¹³E. Fawcett, Phys. Rev. Lett. **26**, 829 (1971).

¹⁴B. T. Matthias, Physica (Utrecht) **69**, 54 (1973).

¹⁵J. M. Vandenberg and B. T. Matthias, to be published.

¹⁶C. W. Chu and L. R. Testardi, Phys. Rev. Lett. **14**, 766 (1974).

¹⁷G. R. Johnson and D. H. Douglass, J. Low Temp. Phys. **14**, 565 (1974). Geller radii are based on the assumption that the structure is stabilized by $A-B$ contacts only, and neglect the influence of $A-A$ intrachain contacts.

¹⁸J. A. Van Vechten, Phys. Rev. B **7**, 1479 (1973).

¹⁹C. W. Chu, to be published.

²⁰A. R. Sweedler, D. G. Schweitzer, and G. W. Webb, Phys. Rev. Lett. **33**, 168 (1974).

²¹T. F. Smith, *Superconductivity in d- and f-Band Metals*, AIP Conference Proceedings No. 4, edited by D. H. Douglass (American Institute of Physics, New York, 1972). See esp. the effects of nonhydrostatic pressure (p. 299) and alloy data (p. 306).